

## Hard QCD Processes at Colliders

Lance J. Dixon  
*Stanford Linear Accelerator Center  
 Stanford University  
 Stanford, CA 94309, USA*

Recent developments in the study of hard QCD processes at colliders are reviewed, in the context of the imminent startup of the LHC.

*Invited talk presented at the XXIII International Symposium  
 on Lepton and Photon Interactions at High Energy (LP07)  
 August 13 - 18, 2007, Daegu, Korea*

### I. INTRODUCTION

Next year, the Large Hadron Collider (LHC) will begin operation at CERN, colliding protons at a center-of-mass energy of 14 TeV, seven times greater than that currently available in  $p\bar{p}$  collisions at Fermilab's Tevatron. The LHC luminosity should also be a factor of 10 to 100 greater than the Tevatron's. The combined rise in energy and luminosity represents the opening of a new window into electroweak-scale physics. There will be copious production of heavy states such as electroweak vector bosons and top quarks, and, it is anticipated, Higgs boson(s) and physics beyond the Standard Model.

Are we ready to exploit this new window? That is, is Standard Model physics at the LHC understood well enough to confidently extract physics beyond the Standard Model? Of course the physics at the LHC *is* largely the physics of hard QCD processes (with important contributions from soft regimes as well). QCD itself will be probed in unprecedented regimes and with unprecedented statistics. QCD governs the production of electroweak states in and beyond the Standard Model. Pure jet final states also need to be understood, because jet production rates are so large. Jets can fake electroweak signatures such as leptons or photons, and can fake missing energy via mismeasurement. In general, QCD (plus electroweak) hard processes form significant backgrounds to almost all new physics searches at the LHC, as well as at the Tevatron.

To be sure that our understanding of hard QCD at the LHC is good enough, it is important to check QCD predictions against current data from the Tevatron and HERA. The main experimental inputs are the strong coupling,  $\alpha_s(M_Z)$ , and the parton distribution functions.

Recent progress in computing three-jet observables in  $e^+e^-$  annihilation at next-to-next-to-leading order (NNLO) [1], to be described below, promises to improve the experimental uncertainty in  $\alpha_s$  as determined from  $e^+e^-$  event shapes. On the other hand, the uncertainty in the current world average [2],

$$\alpha_s(M_Z) = 0.1182 \pm 0.0027, \quad (1.1)$$

is already small, in comparison with other uncertainties, for almost all LHC processes. Parton distribution functions (pdfs), and their uncertainties, are critical to all QCD predictions, but as they were reviewed in the talks by Gwenlan [3] and Diehl [4], I will not dwell on them here. Here I will focus more on our theoretical understanding of the hard, short-distance structure of QCD processes, assessed when possible against Tevatron and HERA data for various processes and regimes.

Because hard QCD is a vast subject, this talk will only scratch the surface. I will say next to nothing about several important subjects covered in part by other speakers, such as the high-energy (BFKL) limit, small- $x$  physics and parton saturation [4]; (hard) diffraction [4, 5]; and heavy quark production [3, 6]. I will also not be able to cover multiple parton scattering and the underlying event; the substantial recent progress in matching leading-order QCD predictions with parton showers; other Monte Carlo developments; insights for collider physics being developed via soft collinear effective theory; and new techniques for computing one-loop QCD amplitudes with many external legs.

Section II of this article outlines the framework and basic elements of fixed-order QCD computations and briefly discusses resummation. Section III describes a state-of-the-art application to  $e^+e^-$  annihilation, the thrust distribution at NNLO [1]. In Section IV, developments in the theory of Higgs production at hadron colliders are summarized, along with selected decay channels and some backgrounds thereof. Section V is devoted to jet physics: definitions, substructure, rates and distributions. Section VI covers the production of a vector boson in association with jets. Section VII discusses the production of a top quark pair plus a jet, and the  $t\bar{t}$  forward-backward asymmetry. In Section VIII I conclude.

### II. PRELIMINARIES AND THEORETICAL TOOLS

Asymptotic freedom in QCD [7] guarantees that at short distances (large transverse momenta) the partons in

the proton are almost free, and are sampled essentially one at a time in hard collisions. This picture leads to the QCD-improved parton model, in which the hadronic cross section for production of a final state  $X$  factorizes into products of pdfs  $f_a$  and partonic cross sections  $\hat{\sigma}^{ab \rightarrow X}$ ,

$$\begin{aligned} \sigma^{pp \rightarrow X}(s; \alpha_s, \mu_F, \mu_R) \\ = \sum_{a,b} \int_0^1 dx_1 dx_2 f_a(x_1, \alpha_s, \mu_F) f_b(x_2, \alpha_s, \mu_F) \\ \times \hat{\sigma}^{ab \rightarrow X}(sx_1 x_2; \alpha_s, \mu_F, \mu_R). \end{aligned} \quad (2.1)$$

Here  $\mu_F$  and  $\mu_R$  are the factorization and renormalization scales, which are in principle arbitrary. In practice, truncating the cross section at a given order in perturbation theory induces dependence on  $\mu_F$  and  $\mu_R$ .

Although parton distributions are nonperturbative quantities which must be measured experimentally at some short-distance scale  $\mu$ , their evolution with  $\mu$  is governed by the DGLAP equation [8],

$$\frac{\partial f_a(x, \mu)}{\partial \ln \mu^2} = \frac{\alpha_s(\mu)}{2\pi} \int_x^1 \frac{d\xi}{\xi} P_{ab}(x/\xi, \alpha_s(\mu)) f_b(\xi, \mu), \quad (2.2)$$

whose kernel is known through NNLO [9],

$$P_{ab}(x, \alpha_s) = P_{ab}^{(0)}(x) + \frac{\alpha_s}{2\pi} P_{ab}^{(1)}(x) + \left(\frac{\alpha_s}{2\pi}\right)^2 P_{ab}^{(2)}(x) + \mathcal{O}(\alpha_s^3). \quad (2.3)$$

The partonic cross section can be expanded similarly in powers of  $\alpha_s$ ,

$$\begin{aligned} \hat{\sigma}^{ab \rightarrow X}(\alpha_s, \mu_F, \mu_R) \\ = [\alpha_s(\mu_R)]^{n_\alpha} \left[ \hat{\sigma}^{(0)} + \frac{\alpha_s(\mu_R)}{2\pi} \hat{\sigma}^{(1)}(\mu_F, \mu_R) \right. \\ \left. + \left(\frac{\alpha_s(\mu_R)}{2\pi}\right)^2 \hat{\sigma}^{(2)}(\mu_F, \mu_R) + \mathcal{O}(\alpha_s^3) \right], \end{aligned} \quad (2.4)$$

where  $n_\alpha$  depends on the process. For typical collider processes,  $\mu_R$  might be of order 100 GeV, for which  $\alpha_s(\mu_R) \approx 0.1$ . One might expect that the leading-order (LO), or Born level, terms in the expansion ( $\hat{\sigma}^{(0)}$ ) would suffice to get a 10% uncertainty. However, for hadron collider cross sections, corrections from the next-to-leading order (NLO) terms in the  $\alpha_s$  expansion ( $\hat{\sigma}^{(1)}$ ) can increase the cross section by 30% to 80%. There are several reasons for the large corrections, some of which we shall discuss below. Thus, LO predictions are only qualitative; quantitative predictions require NLO corrections. If a few percent precision is desired, then the next-to-next-to-leading order (NNLO) terms, may also be required. Also one must be careful to describe the experimental setup (cuts, *etc.*) sufficiently accurately.

## A. Basic ingredients at fixed order

What ingredients enter a perturbative QCD calculation at LO, NLO, or NNLO? First of all, various partonic scattering amplitudes are required. These amplitudes are illustrated in fig. 1 for one of the simplest processes, the inclusive production of a  $Z$  boson at a hadron collider, followed by  $Z$  decay to an electron-positron pair. At LO, only tree amplitudes are needed. In this example, a single Feynman diagram contributes to  $q\bar{q} \rightarrow Z \rightarrow e^+e^-$ . This diagram just needs to be squared, and convoluted with the pdfs, while incorporating any experimental cuts on the final state leptons.

At NLO, one-loop amplitudes contribute to virtual corrections; for example, the one-loop correction to  $q\bar{q} \rightarrow Z$ . The virtual corrections must be combined with real radiation; *i.e.*, tree amplitudes having one additional parton in the final state. In the  $Z$  example, the subprocesses are  $q\bar{q} \rightarrow Zg$ ,  $qg \rightarrow Zq$  and  $\bar{q}g \rightarrow Z\bar{q}$ . The virtual and real corrections are separately divergent in the infrared (IR), which includes both soft and collinear regions. Usually the IR divergences are regulated dimensionally, by letting the number of spacetime dimensions be  $D = 4 - 2\epsilon$  (with  $\epsilon < 0$ ), and expanding both virtual and real contributions in a singular Laurent expansion around  $\epsilon = 0$ . There are  $1/\epsilon^2$  singularities that cancel between virtual corrections and real corrections. Some of the  $1/\epsilon$  singularities also cancel this way; others, representing initial-state collinear singularities, are absorbed into a renormalization of the pdfs. Ultraviolet poles are removed by coupling renormalization. The finite remainder is then convoluted with the pdfs, as at LO.

At NNLO, there are three types of terms: two-loop virtual corrections to the lowest-order process; mixed virtual/real corrections from one-loop amplitudes with one additional parton; and tree amplitudes with two additional partons, as shown in fig. 1. The IR cancellations are increasingly intricate, beginning now at order  $1/\epsilon^4$ .

As the number of final-state partons in a process grows, the complexity of the theoretical computation increases, at every order in  $\alpha_s$ , but the issue is particularly problematic at NLO and NNLO. Consider, as an example, the processes  $pp \rightarrow n$  jets. At LO, fast numerical programs allow the computation of the  $n$ -jet final-state up to about 8 jets [10], depending on the computing time available. At NLO, there are no complete results for more than three jets. In this case, the main limitation is the lack of knowledge of the one-loop amplitudes for more than five external partons (except for one case,  $gg \rightarrow gggg$ ). At NNLO, even the basic two-jet final state cannot yet be computed at NNLO. Here the required amplitudes are all known, and the main obstacle has been the integration over the singular final-state phase space. More interesting final states may include electroweak particles such as  $W$ ,  $Z$ , or Higgs bosons in addition to jets. In each case, the state-of-the-art value of  $n$  is the same or smaller as in the  $n$ -jet case, if one counts each electroweak particle as replacing one jet.

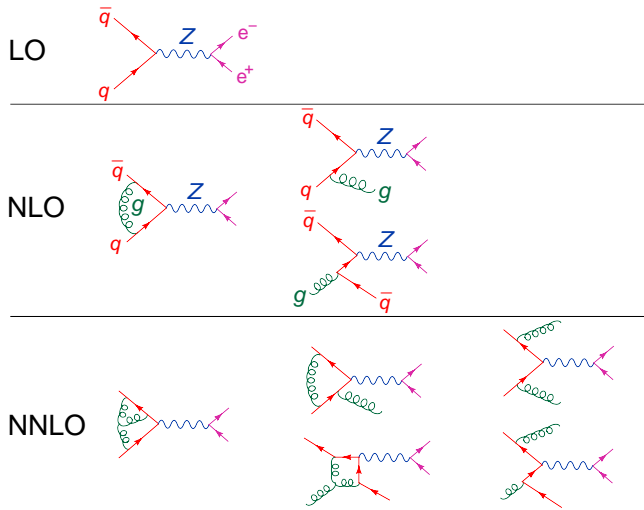


FIG. 1: Sample Feynman diagrams contributing to  $Z$  boson production at a hadron collider, at LO, NLO, and NNLO. Only one diagram is shown for each contributing amplitude, and some amplitudes are omitted.

## B. Singular phase-space integration

Most of the recent advances in computing NNLO corrections to collider processes have come from the development of methods for integrating over singular regions of phase space where one or two partons are “unresolved”, *i.e.*, are either soft or are collinear with another, hard parton. There have also been recent advances at NLO, in the context of matching parton showers with fixed-order computations, which exploit an understanding of the singular phase-space structure.

At NLO, only one parton can be unresolved. For example, consider the final-state gluon in the tree-level amplitude for  $q\bar{q} \rightarrow Zg$  in fig. 1. There is a soft singularity when the gluon momentum vanishes,  $k_g \rightarrow 0$ . This singularity can be interpreted classically, as radiation from the “accelerating” quark color charges when the quark and antiquark annihilate. Thus soft radiation is associated with a pair of external partons. There are also two collinear singularities, one in which the gluon is collinear with the quark, from the Feynman diagram shown in fig. 1; and one in which the gluon is collinear with the antiquark, from another Feynman diagram (not shown).

Various techniques have been developed for handling these singular integrals at NLO, and some of them are also being applied at NNLO. There are four general categories of methods:

- **analytic** — Usually carried out on a case-by-case basis, for the simplest processes only, with (at best) very simple cuts.
- **slicing** [11] — Thin strips are excised from the singular regions of phase space. An approximate version of the cross section can be integrated analytically in the strips. Outside the strips, the integral

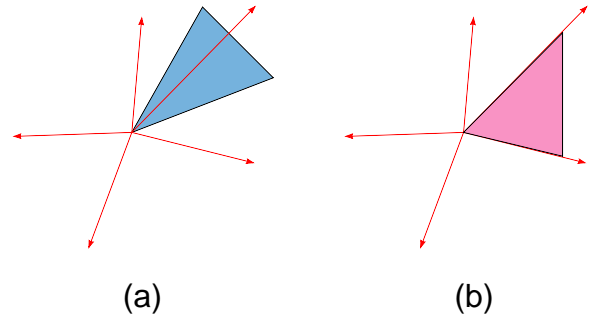


FIG. 2: Schematic depiction of two different types of subtraction methods. Arrows represent momenta of hard external partons. (a) The dipole subtraction method is built around collinear singularities associated with individual partons. (b) The antenna subtraction method is built around soft singularities associated with pairs of partons.

is finite, so it can be performed numerically, with generic experimental cuts.

- **subtraction** [12, 13, 14, 15, 16, 17] — One subtracts, over the entire phase space, a function mimicking the exact cross section in singular regions, but which can be integrated more easily, even in the presence of cuts. The subtracted difference is integrated numerically.
- **direct numerical integration** [18, 19, 20] — This approach can be carried out for a variety of processes, even at NNLO, but most effectively after using sector decomposition [21] to help separate the singularities.

Within the category of subtraction methods, one can distinguish two different ways of building up subtraction terms for general processes out of simpler building blocks. The problem is that soft singularities connect all possible pairs of legs, while collinear singularities are associated with individual legs. Also, soft and collinear regions overlap, so any smooth subtraction term should have a soft part and a collinear part. Figure 2(a) sketches the building block for the *dipole subtraction* method [15]. This function captures the collinear behavior near a particular hard parton, plus part of the soft behavior connecting that parton to other color-correlated partons.<sup>1</sup> Figure 2(b) illustrates the building block for the *antenna subtraction* method [16]. It captures the soft behavior associated with a pair of color-connected partons, plus part of the collinear behavior near each of the members of the pair.

<sup>1</sup> The term “dipole” used here differs from the “dipole shower” used in the Monte Carlo community, which is closer to an antenna pattern.

### C. Parton showers and NLO matching

Parton showers represent an approximation to the soft and collinear radiation pattern, a resummation of leading logarithms (at present), which can be implemented probabilistically. Parton showers are a key part of Monte Carlo simulation programs such as `PYTHIA` [22] and `HERWIG` [23], which produce hadron-level events and are essential to experimental analyses. To improve the accuracy of parton-shower Monte Carlo programs, it is important to match them to fixed-order results. LO matching is an important subject which I cannot do justice to here; see however, ref. [24] for a recent comparative study of different approaches.

For even better accuracy, though, NLO matching is necessary. The program `MC@NLO` [25] was the first to accomplish NLO matching for a variety of different processes. It operates within the `HERWIG` Monte Carlo, which uses an angular-ordered shower. Implementing additional processes in `MC@NLO` has been nontrivial. An important issue is to avoid the double-counting of emissions, between (i) the first step of the shower, and (ii) the exact radiation pattern in QCD, from which subtraction terms have been removed in the course of the NLO computation. If the shower radiation pattern differs from the form of the subtraction terms, a correction is necessary.

Recently there have been some advances in achieving NLO matching in a more process-independent way. The `POWHEG` method [26], in contrast to `HERWIG`, generates the hardest parton emission first, and works well with  $p_T$ -ordered showers. Recently it has been formulated for a general NLO subtraction method, and in particular for the Frixione-Kunszt-Signer [14] and dipole [15] methods, for generic processes [27].

It has also been recognized [28] that subtraction methods automatically supply radiation patterns that are correct in the soft and collinear limits, and hence can be used to construct a parton shower. In this case the double-counting problem is solved automatically, because the first step of the shower coincides with the NLO subtraction function. Two independent implementations of a shower based on dipole subtraction have appeared very recently [29], as well as one (`VINCIA`) based on antenna subtraction [30]. With the recent flourishing of different parton-shower algorithms and NLO matching routines, it will be very interesting to compare their outputs for benchmark processes over the next year or two.

### D. Subtraction at NNLO

Let us return now to the status of fixed-order results. The NLO technique that has been carried out for the widest variety of collider processes is the dipole subtraction method. Programs such as `MCFM` [31] and `NLOJET++` [32] cover a variety of hadron collider,  $ep$  collider and  $e^+e^-$  processes, limited mainly by the availability of virtual corrections (one-loop amplitudes). The

method has been generalized to handle massive final-state partons (such as top quarks) [33]; and a fully automated version of the method in the massless case has appeared very recently [34].

It is natural to try to generalize this method to NNLO. Such a generalization is highly non-trivial, because there are now several different types of singular phase-space regions, for the contributions with two additional radiated partons, exemplified by the rightmost terms on the NNLO line in fig. 1. There can be singularities when both additional partons are soft, when one is soft and the other collinear; when both are collinear with a third parton; and when there are two independent collinear pairs. These different regions overlap with each other. Nevertheless, progress has been made in constructing dipole-type subtraction terms for  $e^+e^-$  annihilation to jets [35]. The method has also been adapted to give NNLO results for the inclusive production of a Higgs boson via gluon fusion at hadron colliders [36].

The most complex process that has been treated to date at NNLO is that of three-jet event shapes in  $e^+e^-$  annihilation, such as the thrust distribution [1] to be described further in the next section. These results relied on building antenna-type subtractions to handle all the singular regions, and evaluating their phase-space integrals [18, 37].

### E. Sector decomposition at NNLO

Iterated sector decomposition is a strategy for doing singular integrals by partitioning the integration region, and then remapping it, in order to make the singularities one-dimensional. A very simple example of the procedure starts with the integral

$$I = \int_0^1 \int_0^1 dx dy \frac{x^\epsilon y^\epsilon}{(x+y)^2}. \quad (2.5)$$

Integrals like  $I$  are encountered in the NNLO corrections to vector boson production (for example), from the interference of two different initial-state radiation graphs in which a parton, radiated from either incoming line, splits into two additional partons. Although  $I$  is not singular as either  $x$  or  $y$  approaches zero with the other variable held fixed, there is a singularity as  $x = y \rightarrow 0$ . This singularity can be exposed by splitting the unit square into sectors  $A$  and  $B$  shown in fig. 3, and then remapping region  $A$  back to the unit square using  $x' = x$ ,  $1 - y' = (1 - y)/(1 - x)$ , and  $B$  back to the unit square using  $y' = y$ ,  $1 - x' = (1 - x)/(1 - y)$ . These transformations map the  $x = y \rightarrow 0$  singularity onto one variable,  $x' \rightarrow 0$  or  $y' \rightarrow 0$ , depending on the sector. This technique was first applied to multi-loop integrals [21], and later to phase-space integrals [18, 19, 20]. Several iterations and many sectors may be required for state-of-the-art NNLO results. The expansion in  $\epsilon$  for one-dimensional singularities is straightforward, involving standard “plus” distri-

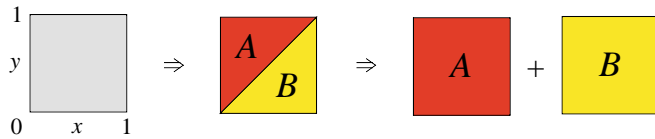


FIG. 3: Sector decomposition splits and remaps integration regions in order to expose multi-variable singularities.

butions. Hence arbitrary observables can be integrated over phase space.

### F. Soft-gluon resummation

In particular kinematic regions, fixed-order perturbation theory breaks down. This breakdown can be due to a mismatch between the kinematics of virtual and real corrections, enhanced by the strength of soft-gluon emission. For example, in  $Z$  production by  $q\bar{q}$  annihilation, the transverse momentum of the  $Z$ ,  $q_T(Z)$ , vanishes for all virtual corrections, but is nonzero for real corrections, which are enhanced for small  $q_T(Z)$ . The leading behavior at  $L$  loops is

$$\frac{d\hat{\sigma}}{dq_T^2(Z)} \sim (C_F\alpha_s)^L \frac{\ln^{2L-1} q_T^2(Z)}{q_T^2(Z)} + \dots \quad (2.6)$$

plus terms with fewer logarithms. Here  $C_F = 4/3$  is the quark color charge. These large corrections imply that *transverse-momentum resummation* [38] is required for  $q_T(Z) \ll M_Z$ .

Distributions in the threshold variable  $z \equiv M_Z^2/s_{q\bar{q}}$  behave similarly. Virtual corrections have  $z = 1$ , while real corrections have  $z < 1$ , and are enhanced as  $z \rightarrow 1$ , with leading behavior,

$$\frac{d\hat{\sigma}}{dz} \sim (C_F\alpha_s)^L \left[ \frac{\ln^{2L-1}(1-z)}{1-z} \right]_+ + \dots \quad (2.7)$$

Such singular distributions can give rise to large corrections to inclusive production cross sections if they are convoluted with steeply falling parton distributions, necessitating *threshold resummation* [39].

The kinematics are similar for production of the Higgs boson via gluon fusion, except that the color charge for gluons,  $C_A = 3$ , is much larger than for quarks, and the gluon pdfs are falling much faster than the quark pdfs in the relevant  $x$  range,  $x \sim 10^{-2}$ . Hence both  $p_T$  and threshold resummation effects are much larger in this case than for vector boson production.

### III. AN $e^+e^-$ APPLICATION – THRUST AT NNLO

Next I turn to some recent applications of these theoretical techniques to collider processes, beginning with

one from  $e^+e^-$  annihilation. The thrust [40] is a classic infrared-safe  $e^+e^-$  event-shape observable, defined by

$$T = \max_{\hat{n}} \frac{\sum_i |\vec{p}_i \cdot \hat{n}|}{\sum_i |\vec{p}_i|}. \quad (3.1)$$

The sum is over the final-state hadrons (or partons, in a perturbative calculation) with spatial momenta  $\vec{p}_i$ , and  $\hat{n}$  is a unit vector, varied over all directions. There is a wealth of data to compare to, for  $\sqrt{s}$  from 14 to 206 GeV, with the best statistics gathered on the  $Z$  pole. In the extraction of  $\alpha_s(M_Z)$  from a fit of NLO QCD predictions to  $e^+e^-$  event shapes, it is a long-standing problem (see *e.g.* ref. [41]) that the central value depends on the observable used, and on the range in that observable used in the fit. The error is dominated by the truncation of the perturbative series at NLO.

Finally, 27 years after the first NLO event-shape results [12], the first NNLO results have appeared this year [1]. At the  $Z$  pole, the effect of the NNLO corrections is to increase the NLO thrust distribution by about 15–20% in the range  $0.04 < 1 - T < 0.33$ . (The two-jet region,  $1 - T < 0.03$ , requires resummation. The region  $1 - T > 0.33$  cannot be produced by  $q\bar{q}g$  final states, so it is also less perturbatively stable.) The relative uncertainty in the perturbative prediction is reduced by about 30–40% with respect to NLO.

The increase in the thrust distribution should lead to a somewhat smaller  $\alpha_s(M_Z)$ ; but at NLO the thrust led to a larger than average value,  $\alpha_s(M_Z) \approx 0.126$ . A new, more precise value of  $\alpha_s(M_Z)$  requires experimental re-analysis, incorporating:

1. a resummation of large logarithms for  $1 - T \rightarrow 0$ ,
2. an analysis of power corrections of the form  $\Lambda_{\text{QCD}}/Q$  using data off the  $Z$  pole,
3. other event-shape observables, which have also been computed (very recently) at NNLO [42].

Indeed, the first NNLO determination of  $\alpha_s$  from event-shape variables, using ALEPH data for six different variables (including thrust) from several center-of-mass energies, has just been reported (post LP07) [43],

$$\alpha_s(M_Z) = 0.1240 \pm 0.0008_{\text{stat}} \pm 0.0010_{\text{exp}} \pm 0.0011_{\text{had}} \pm 0.0029_{\text{theo}}. \quad (3.2)$$

The result is a bit higher than the world average (1.1). The perturbative uncertainty, “theo”, has been cut roughly in half with respect to NLO. Further analyses, incorporating resummation and power corrections, are eagerly awaited!

## IV. HIGGS PRODUCTION AT HADRON COLLIDERS

### A. Gluon fusion total cross section

Let's begin the discussion of hadron collider applications with Higgs boson production and decay. These results are of great phenomenological importance for the Higgs search at the Tevatron, and particularly at the LHC. The gluon-fusion channel,  $gg \rightarrow H$ , via a top quark loop, represents one of the simplest final states, apart from vector boson production, so the theory has already been pushed to rather high order. At the same time, the process illustrates methods of analysis that should eventually be applied to more complex states.

In the most likely mass range for the Standard Model Higgs boson, from 114 GeV to about 200 GeV, gluon fusion dominates the total production cross section  $\sigma_H$ . It has been known since the early 1990s that the NLO corrections to  $\sigma_H$  were huge, increasing it by roughly 80% [44]. Because the lowest-order process proceeds by a loop diagram, the NLO corrections already require two-loop integrals. To go to NNLO, the large- $m_t$  approximation has been used. This approximation shrinks the top-quark triangle to a point, replacing it by an effective operator,  $H G_{\mu\nu}^a G^{\mu\nu a}$  [45], with coefficient  $C_H$ . It reduces the number of loops and the number of mass scales in the problem by one. This makes it feasible to perform all the NNLO computations, including the phase-space integrals, analytically for the case of inclusive production [46]. Threshold logarithms, of the form

$$\frac{d\hat{\sigma}_H}{dz} \sim (C_A \alpha_s)^L \left[ \frac{\ln^k(1-z)}{1-z} \right]_+, \quad (4.1)$$

with  $k = 0, 1, \dots, 2L - 1$ , play a big role in the large positive corrections. They have been resummed to next-to-next-to-leading logarithmic (NNLL) accuracy [47]. Nevertheless, a sizable uncertainty of order 10–15% remained in the prediction.

Some progress has been made on reducing this uncertainty. As a spinoff from the computation of the NNLO DGLAP kernel for gluon evolution,  $P_{gg}^{(2)}(x)$  [9], Moch and Vogt [48] were able to extract the leading singular terms (4.1) at three loops,  $L = 3$  and  $k = 0, 1, 2, 3, 4, 5$ . They defined an approximation  $N^3LO_{\text{approx}}$  which is missing just the  $\delta(1-z)$  term, plus all terms that are nonsingular as  $z \rightarrow 1$ . They also employ the  $N^3LO$  corrections to the coefficient  $C_H$  [49]. The results are shown in fig. 4. The renormalization-scale dependence is now stabilized near the Higgs mass, with a residual uncertainty of order 5%. More recently, a similar analysis has been carried out at order “ $N^4LO_{\text{approx}}$ ” with the six leading terms in eq. (4.1) at that order [50]. The results change by about 2% with respect to the  $N^3LO_{\text{approx}}$  results shown in the figure. The total Higgs production cross section is now becoming a precision observable.

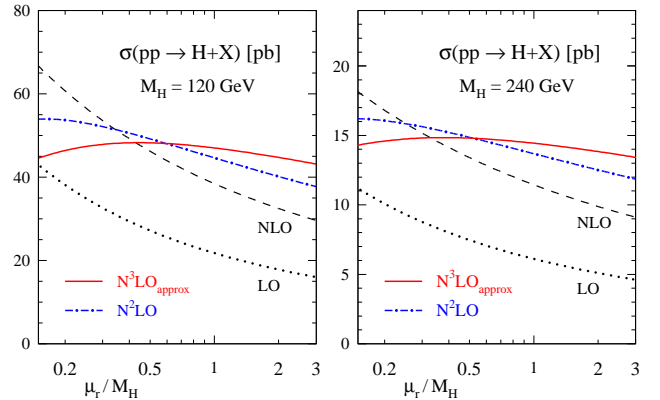


FIG. 4: Variation of the total Higgs production cross section with respect to the renormalization scale  $\mu_r$ , at various levels of approximation. Figure from ref. [48].

### B. Gluon fusion with decay to two photons

Unfortunately, the total Higgs production cross section cannot be observed experimentally. For any final state, various experimental cuts have to be imposed. For example, for the two-photon final state from the decay  $H \rightarrow \gamma\gamma$  there are cuts on the photons' transverse momentum, rapidity, and isolation (with respect to hadronic energy). These cuts can now be mimicked at the parton level at NNLO, for gluon fusion production (in the large- $m_t$  limit) followed by  $H \rightarrow \gamma\gamma$ . (The same is now also true for the decay mode  $H \rightarrow WW \rightarrow \ell\nu\ell\nu$  [36, 51].) Two independent programs are available for the  $\gamma\gamma$  final state. The program FEHiP [20] uses direct numerical integration, following sector decomposition for the real corrections. The more recent program HNNLO [36] employs a subtraction method, based on the fact that at nonzero Higgs  $q_T$  the problem is really a NLO calculation; plus a knowledge, based on resummation studies, of the universal behavior of the  $q_T$  distribution as  $q_T \rightarrow 0$ .

For regions of final-state phase space that are accessible at LO, both programs show good perturbative stability in going from NLO to NNLO. However, the behavior near boundaries of the LO-accessible region is more unstable, again reflecting the breakdown of fixed-order perturbation theory. One such boundary occurs at a large rapidity difference between the two photons [20]. At  $q_T = 0$ , the photon  $p_T$  cuts and fixed Higgs mass  $m_H$  put a bound on how forward and backward the decay photons can go. More obvious boundaries occur in the transverse momenta of the two photons,  $p_{T\text{min}}$  and  $p_{T\text{max}}$ , which each have to be less than  $m_H/2$  at LO. One can see from fig. 5 that the  $p_{T\text{max}}$  distribution gets significantly stiffer, and the  $p_{T\text{min}}$  distribution gets softer, from NLO to NNLO [36]. (The distributions are forced to be identical at LO.)



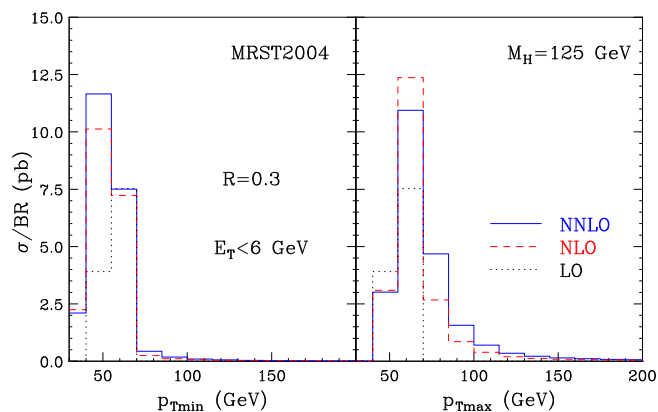


FIG. 5: Distributions of transverse momenta  $p_T$  for the minimum and maximum  $p_T$  photons for Higgs production at the LHC, followed by the decay  $H \rightarrow \gamma\gamma$ , at LO, NLO and NNLO. Figure from ref. [36].

### C. The two-photon background

In searching for a bump from the Higgs boson in the invariant-mass of photon pairs, it is also useful to know the characteristics of the continuum QCD background. The  $\gamma\gamma$  background has many components, including:

- electrons, positrons and hadrons faking photons
- photons arising from copious  $\pi^0$  decays and electron or positron bremsstrahlung
- photons arising from fragmentation — radiation at small transverse momentum with respect to a jet
- hard QCD radiation of photons.

The first three categories of backgrounds can be suppressed fairly effectively by photon isolation cuts.

Direct production of photon pairs in hard QCD begins at LO with the quark-annihilation process  $q\bar{q} \rightarrow \gamma\gamma$ . The process  $qg \rightarrow \gamma\gamma q$  enters at NLO. It is heavily enhanced, by the large gluon pdf at small  $x$ , and by a final-state collinear singularity between each photon and the outgoing quark. (At very small angles, the singularity is absorbed into the fragmentation contribution; it is also suppressed by isolation cuts.) At NNLO, the process  $gg \rightarrow \gamma\gamma$ , mediated by a virtual quark loop, enters for the first time. It is significant, however, because the gluon pdf enters twice. NLO programs for the inclusive di-photon background, including fragmentation effects, were constructed in the late 1990's [52, 53]. The contribution from the  $gg \rightarrow \gamma\gamma$  subprocess at *its* next-to-leading order in the pdf-enhanced channel  $gg \rightarrow \gamma\gamma(g)$  was added a few years later [54]. This year the quark-box contribution to  $qg \rightarrow \gamma\gamma q$  was included, as well as a resummation of the transverse momentum  $q_T$  of the di-photon pair at NNLL accuracy [55, 56].

CDF has presented  $207 \text{ pb}^{-1}$  of data [57] on pairs of photons produced at the Tevatron with  $p_T^\gamma > 14 \text{ GeV}$

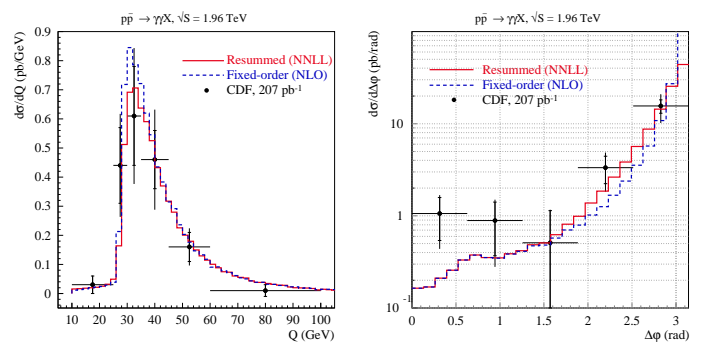


FIG. 6: Distributions in invariant mass  $Q$  and azimuthal angle separation  $\Delta\phi$ , for pairs of photons produced at the Tevatron. Figure from ref. [56].

and di-photon invariant masses ranging from 10 to 100 GeV. This range is useful for assessing the hard QCD background to the Higgs search at the LHC. If one scales a di-photon invariant mass of, say, 150 GeV, and typical photon  $p_T$  cut of 40 GeV, down by the ratio of beam energies between the LHC and the Tevatron (seven), one gets a di-photon invariant mass of order 20 GeV, and  $p_T$  cut of 6 GeV, not too far from the CDF cuts. So similar ranges of  $x$  values for the pdfs are being sampled. Figure 6 shows the CDF data, in comparison with the NLO plus NNLL-resummed predictions [56]. The agreement is generally quite good, within the available statistics, except for the region of small  $\Delta\phi$ . Significant contributions to the small  $\Delta\phi$  region can arise when a single parton yields both photons, *e.g.*  $gq \rightarrow gq\gamma$ , with hard photon radiation off the final-state quark, followed by the fragmentation of that quark to a second photon. These fragmentation contributions are NLO (order  $\alpha^2\alpha_s$ ), and are not included in the computation of ref. [56]. They have been included in the program DIPHOX [53], which does fit the CDF data at small  $\Delta\phi$ . The small  $\Delta\phi$  region will probably not be too important for the Higgs search; such large boosts are kinematically disfavored.

In general, then, the di-photon background at the LHC seems to be in relatively good shape; although a computation of the  $qg \rightarrow \gamma\gamma q$  channel at *its* NLO, leading eventually to a computation of  $q\bar{q} \rightarrow \gamma\gamma(gg)$  at NNLO, would certainly be welcome.

### D. Vector boson fusion

The second largest Higgs boson production mechanism, weak boson fusion (WBF),  $qq \rightarrow qqH$ , features a pair of forward tagging jets, as shown in fig. 7(a). The NLO QCD corrections that dominate in the forward limit are sketched in fig. 7(b). They only involve one quark line at a time, and have been known for a while to be quite modest, only 5% or so [58, 59]. Recently, the complete set of QCD corrections to WBF were computed, as well as the one-loop electroweak corrections to all channels [60].

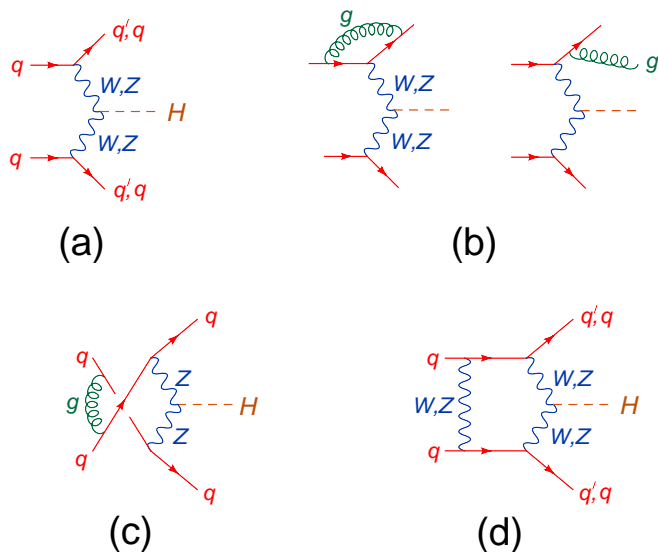


FIG. 7: (a) LO diagram for weak boson fusion. (b) Most important NLO QCD corrections. (c) Example of an additional NLO QCD correction. (d) Sample NLO electroweak correction.

An example of an additional QCD correction is shown in fig. 7(c); it can interfere with the graph in fig. 7(a) if the two quarks are identical. There are also  $s$ -channel annihilation graphs. However, these contributions are kinematically disfavored after typical WBF cuts (emphasizing forward jets) are imposed. Ref. [60] confirms that these contributions are tiny. On the other hand, the one-loop electroweak corrections are found to be sizable and negative, of order  $-7\%$ , so they must be included along with the QCD corrections.

Higgs boson production via WBF has various backgrounds, of course, depending in general on the decay mode. It also has a source of “background” that is independent of the decay mode, coming from the production of a Higgs boson via the gluon fusion subprocess ( $Hgg$  interaction), plus the radiation of at least two more jets. This “background” could in principle impact studies of the WBF production mechanism. While most of the gluon-fusion-plus-two-jets background is eliminated by WBF cuts, it is important to understand how various distributions for this subprocess are affected by higher-order QCD corrections. Recently, gluon-fusion-plus-two-jets was computed at NLO, in the large- $m_t$  limit [61]. The computation employed a semi-numerical evaluation of the one-loop virtual corrections [62]. The overall rate for this subprocess, with typical WBF cuts, increases by 30% in going from LO to NLO. This increase is much less than that for the inclusive gluon-fusion process, but still significant. The azimuthal separation  $\Delta\phi$  of the two tagging jets is an incisive probe of the WBF production mechanism [59]. Figure 8 shows how this distribution changes in going from LO to NLO, in the gluon-fusion-plus-two-jets “background” subprocess. The normalized

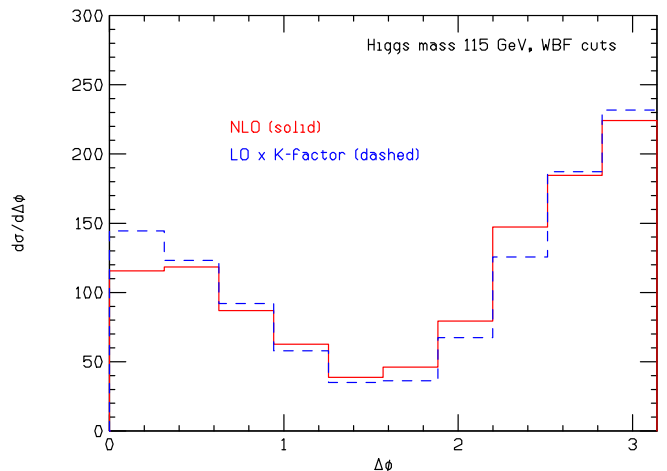


FIG. 8: Distribution in azimuthal separation  $\Delta\phi$  for tagging jets in the gluon-fusion-plus-two-jets process, after applying WBF cuts, at LO (multiplied by the NLO K-factor), and at NLO. Figure from ref. [61].

distribution is fairly stable, only flattening slightly.

## V. JETS

### A. Jet definitions

Jets are by far the most copious high-transverse-momentum objects produced at hadron colliders. They are common as well to almost all  $ep$  final states and a majority of  $e^+e^-$  final states at high energy. Hence a thorough understanding of their production rates and properties in various regimes is highly desirable.

There are two popular classes of algorithms for defining jets. At  $e^+e^-$  colliders, *cluster* algorithms have traditionally been used [63]. A “distance” metric is defined between pairs of particles, which vanishes when the two particles are collinear or one is soft. The pair with the smallest distance is clustered into a proto-jet, and the process is iterated, until all proto-jets are separated by more than a specified distance, called the jet resolution parameter  $y$ . This “bottom up” procedure automatically assigns every particle to a jet. It is *infrared-safe* at the parton level: Adding an arbitrarily soft gluon, or splitting one parton into two very collinear partons, does not change any of the subsequent clustering steps, so the final set of jets remains the same. This means that jet rates can be calculated (in principle) to any order in perturbation theory.

Events at hadron colliders typically contain, in addition to a hard partonic scattering process, an “underlying event”, consisting of forward beam remnants and particles produced more centrally by interactions of spectator partons with each other and with partons from the hard process. The  $k_T$  algorithm [64] is a cluster-style algorithm that has been adapted for use at both  $ep$  and



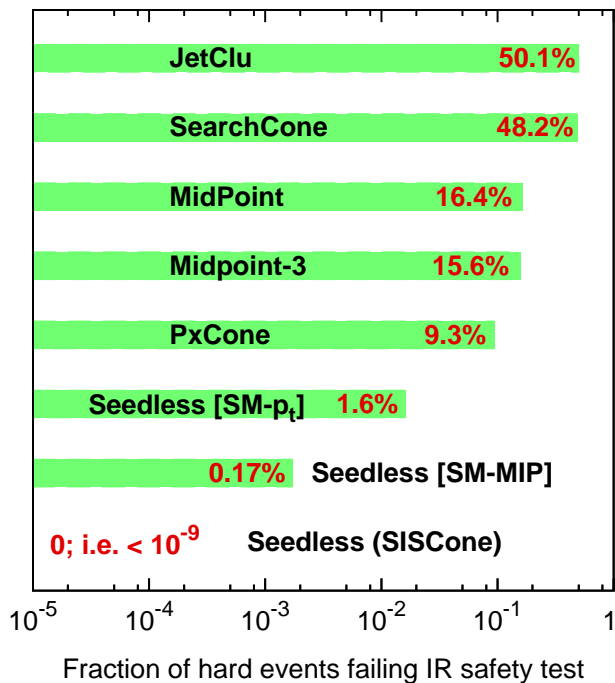


FIG. 9: Fraction of hard events that fail an infrared-safety test, for various cone algorithms. Figure from ref. [68].

hadron colliders. It clusters particles that are “closer” to the beam axis into a beam jet, rather than into one of the other jets. However, some energy from the underlying event will still be associated with non-beam jets, and quantifying this is an issue, although it can be done [65].

Traditionally, hadron collider jet algorithms have been based instead on *cones*. Cone jets are circles of fixed radius  $R$  in the plane of pseudorapidity  $\eta$  and azimuthal angle  $\phi$  containing a set of final-state hadrons, or a set of calorimeter towers, with total transverse momentum  $p_T^{\text{jet}}$  above a particular lower threshold. There are also rules for splitting and merging nearby cones in order to arrive at a stable configuration. Usually the cones are “seeded”; *i.e.*, there is a prescription for specifying which circle centers will be considered first. The seeds might be towers with transverse momentum above a seed threshold. Minimum-bias events distribute energy uniformly in the  $\eta$ - $\phi$  plane, making for a simple prescription for correcting for the underlying event in a cone algorithm. See *e.g.* refs. [66, 67] for more details.

Unfortunately, for seeded cones there is a danger of infrared unsafety: The final jet configuration can sometimes change by a lot, with the addition of an arbitrarily soft gluon. Introducing a midpoint seed between all the previous seeds can reduce the problem, but not eliminate it. In the past year, a new, computationally practical, seedless cone algorithm, SIScone, was invented [68]. This algorithm is infrared safe, as shown in fig. 9. The figure also indicates the fraction of hard events that fail an infrared-safety test, for some other popular cone algorithms.

Packages are now available that give the user the flexibility to reconstruct jets with a variety of algorithms and parameters, and to do comparisons of jet properties between different algorithms [67, 68, 69].

## B. Jet substructure

To what extent can the identities of underlying partons be deduced from properties of the jets they produce? In particular, can we distinguish light quark jets from gluon jets? It is not possible to do this event by event; however, it is possible to do it statistically, by studying how energy is distributed within the jet. In more detail, event kinematics are used to select gluon-rich or gluon-depleted samples of jets. For these samples, one can measure the distributions of the jet-shape function  $\Psi(r/R)$  — the fraction of energy for a jet with cone size  $R$  that is found in a smaller cone with  $r < R$ . If the distributions differ for the gluon-rich and gluon-depleted samples, then one could use the jet-shape distributions to separate quark and gluon jets, statistically. (Similar studies have been carried out in the past using sub-jet multiplicities, in  $e^+e^-$  [70],  $ep$  [71] and  $p\bar{p}$  [72] collisions.)

In  $p\bar{p}$  collisions, CDF studied the dependence of the jet-shape distribution on the transverse momentum of jets reconstructed with the midpoint algorithm ( $R = 0.7$ ) [73]. Higher transverse-momentum jets are gluon-depleted, in comparison with lower transverse-momentum jets. Good agreement was found with PYTHIA [22], for transverse momenta ranging from 50 GeV (73% gluon, 27% quark, according to PYTHIA;  $\langle \Psi(0.3/R) \rangle = 0.705 \pm 0.015$ ) all the way up to 350 GeV (20% gluon, 80% quark;  $\langle \Psi(0.3/R) \rangle = 0.93 \pm 0.02$ ).

Recently, ZEUS studied the jet-shape distribution in  $ep$  collisions, with 368 pb<sup>-1</sup> of data, using two-jet events and taking the lowest transverse-momentum jet in order to select a gluon-enriched sample [74]. Figure 10 shows the ZEUS data, using the  $k_T$  algorithm with resolution parameter  $D = 2.5$  and jet transverse momenta in the narrow range between 14 and 17 GeV. The agreement with NLO predictions (from the program DISENT[15]) is excellent, to within a percent or so. Thus the substructure of jets in generic events in both  $p\bar{p}$  and  $ep$  collisions is understood very well now.

## C. Inclusive jet rates

The production rate for very high transverse-momentum jets at the Tevatron provides a direct test of QCD interactions at the shortest possible distance scales. Of course, the rate also depends on the parton distribution functions, in particular the large- $x$  gluon distribution. Because jet production rates are rapidly-falling functions of  $p_T$ , they are very sensitive to the jet energy scale calibration, as well as to tails in the jet energy resolution. Both DØ and CDF have presented new

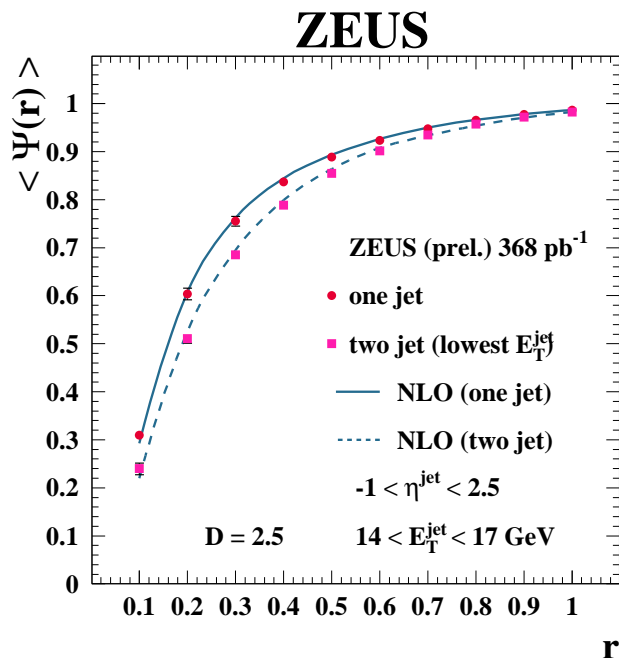


FIG. 10: Jet-shape distribution in  $ep$  collisions for jets in one-jet events, *vs.* the lowest  $p_T$  jet in two-jet events, at the same jet  $p_T$ . Figure from ref. [74].

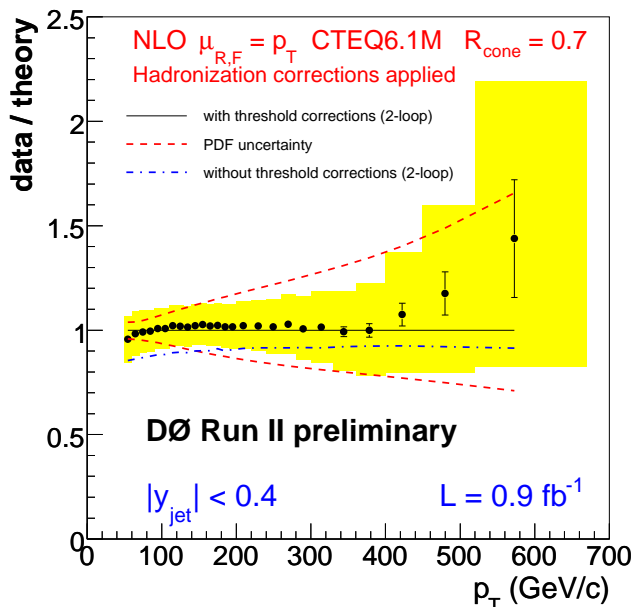


FIG. 11: Ratio of inclusive-jet data from DØ to theory for the midpoint cone algorithm ( $R = 0.7$ ) and central jets, plotted versus transverse momentum  $p_T$ . Figure from ref. [75].

measurements of inclusive-jet rates using midpoint cone algorithms with a cone radius of  $R = 0.7$ , and based on approximately  $1 \text{ fb}^{-1}$  of data.

Figure 11 shows data from DØ divided by theory, for

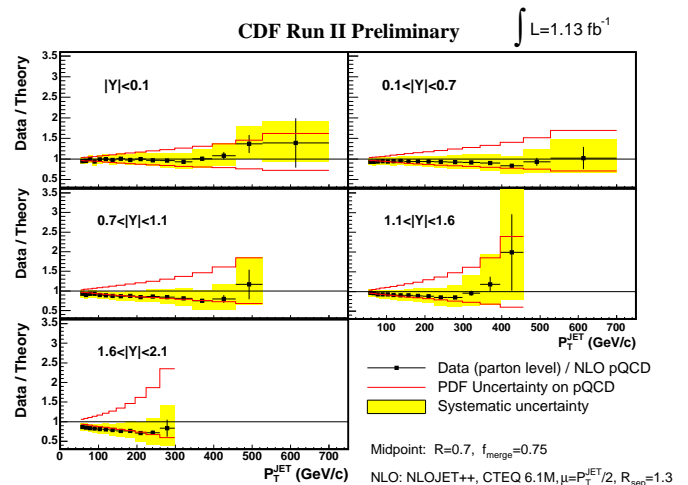


FIG. 12: Ratio of inclusive-jet data from CDF to NLO theory for the midpoint cone algorithm ( $R = 0.7$ ), plotted versus  $p_T$  for various bins in rapidity  $Y$ . Figure from ref. [77].

central jets ( $|y_{\text{jet}}| < 0.4$ ) and binned in  $p_T$ . The theory includes NLO, plus an estimate of the NNLO terms based on threshold logarithms computed at next-to-leading logarithmic (NLL) accuracy [76]. NLO theory without these corrections is about 10% lower in this  $p_T$  range. The central value of the cross section from DØ is closer to the threshold-enhanced theory; however, the systematic uncertainty is too large to distinguish the two curves. Figure 12 shows that the analogous data from CDF [77] is also in good agreement with NLO theory [32], at both central and forward rapidities.

For both the DØ and CDF results, the systematic uncertainty is dominated by the jet energy scale uncertainty and exceeds the statistical error for essentially all points. However, the uncertainty arising from the pdfs is even larger, and increases with  $p_T$ . This fact illustrates that the high- $p_T$  jet data provide a strong constraint on pdfs, and can be used to reduce the pdf uncertainties in particular regimes, particularly the gluon distribution  $g(x)$  at large  $x$ .

#### D. Di-jet azimuthal distributions

At leading order in QCD, two jets produced in a  $p\bar{p}$  collision should emerge back-to-back in the plane transverse to the beam axis, *i.e.* with the maximum azimuthal angle between them,  $\Delta\phi = \pi$ . QCD radiation pushes the azimuthal angle to smaller values. In a multi-jet event, the azimuthal angle is defined to be between the two highest  $p_T$  jets. For  $\Delta\phi \approx \pi$ , multiple soft gluon radiation dominates, and fixed-order perturbation theory cannot be trusted. Because of the way the azimuthal angle is defined, three parton final-states can only produce  $\Delta\phi > 2\pi/3$ . The  $\Delta\phi$  distribution is an excellent test of how well QCD describes complex hadronic final

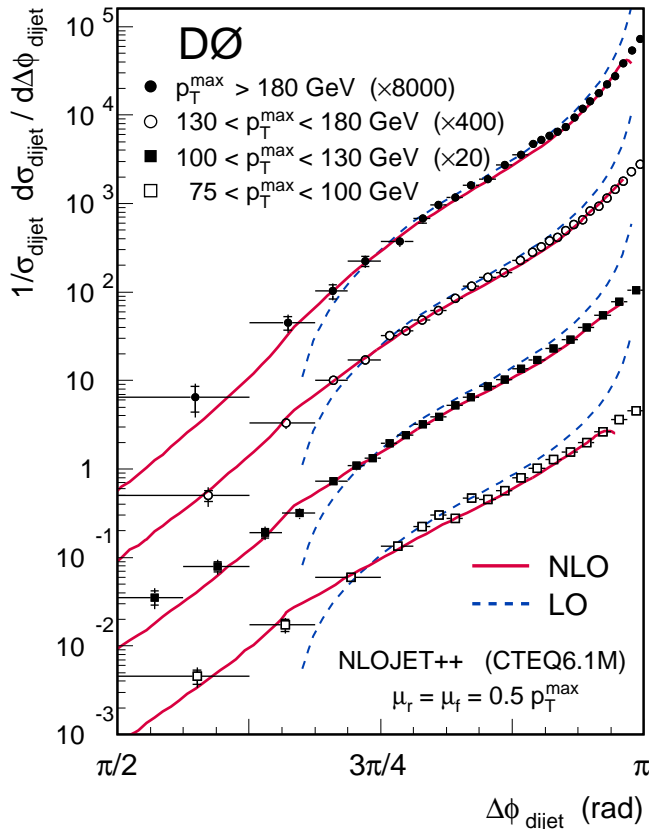


FIG. 13: Distribution in azimuthal angle  $\Delta\phi$  between the two highest- $p_T$  jets in an event, measured by DØ for various  $p_T$  ranges, and compared with LO and NLO QCD. Figure from ref. [78].

states, because it is relatively insensitive to the overall jet energy scale and to the pdfs.

Figure 13 shows DØ’s measurement of the azimuthal decorrelation in di-jet events at the Tevatron [78], compared to LO and NLO predictions from NLOJET++ [32]. LO theory fails for both small and large values of  $\Delta\phi$ , for the reasons mentioned above. However, NLO theory does very well for  $\Delta\phi < 2\pi/3$  (even though it is effectively an LO calculation in this regime), and also pushes the agreement for large values considerably closer to  $\pi$ .

In contrast, NLO theory is unable to describe the azimuthal correlations measured in  $ep$  collisions by H1 [79], shown in fig. 14, at least for small values of  $x_{Bj}$ . The NLO three-jet predictions [80] are closer to the data than are the two-jet predictions, but they still do not produce enough decorrelation at small  $x_{Bj}$ . Does this signal a breakdown of fixed-order perturbation theory for these kinematics, and a need for small- $x$  resummation? Perhaps. On the other hand, H1 also compared the data with a few different models incorporating small- $x$  resummations, and all such models were found to be too low for small  $\Delta\phi$  as well.

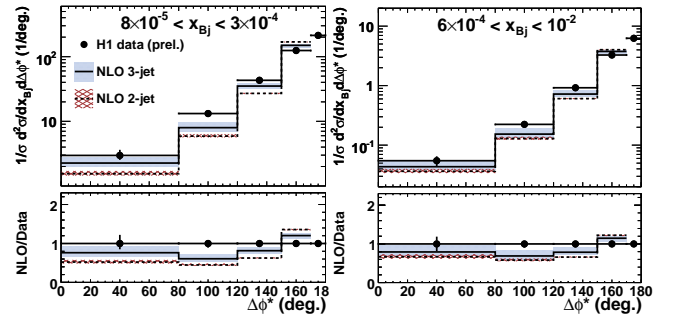


FIG. 14: Azimuthal decorrelations from H1 in the forward region. Figure from ref. [79].

## VI. VECTOR BOSONS PLUS JETS

The production of a single vector boson in association with multiple jets is a background to searches for supersymmetry at the LHC. For example, the final state  $Z + n$  jets, when the  $Z$  decays to  $\nu\bar{\nu}$ , is a background to the missing-transverse-momentum plus multi-jet searches. CDF and DØ have studied such events at the Tevatron, for the decays  $W \rightarrow \ell\nu$  and  $Z \rightarrow \ell^+\ell^-$ , plus up to 4 jets in the final state [81]. Recently, CDF presented data [82] on  $Z$  plus 1, 2 and 3 jets, in comparison with fixed-order LO and NLO predictions. Figure 15 shows the excellent absolute agreement, to within 10%, with NLO predictions for 1 and 2 jets, the maximum number for which NLO results are currently available [83]. These results highlight the importance of extending NLO theory to larger numbers of jets, in order to be ready for the enormous data sets that will be available in these channels at the LHC.

## VII. TOP QUARKS PLUS JETS

The final-state  $t\bar{t}$ +jet is another important background to supersymmetry at the LHC. The cross section is large, and the additional jet can boost the  $t\bar{t}$  system so that neutrinos from top quark decay generate large missing transverse momentum. The NLO corrections to this process were computed recently [84]. They require the evaluation of many virtual Feynman diagrams, including pentagon diagrams with massive propagators, and a large number of subtraction terms for the real corrections [33]. The results greatly reduce the uncertainty on the  $t\bar{t}$ +jet cross section at the LHC.

At the Tevatron, a  $p\bar{p}$  collider, the forward-backward asymmetry of  $t\bar{t}$  pairs is an interesting observable that probes the dynamics of top quark production. It can be defined by

$$A_{\text{FB}}^t = \frac{N_t(y_t > 0) - N_t(y_t < 0)}{N_t(y_t > 0) + N_t(y_t < 0)}, \quad (7.1)$$

where  $N_t(y_t > 0)$  is the number of top quarks produced with positive rapidity. This quantity vanishes at leading

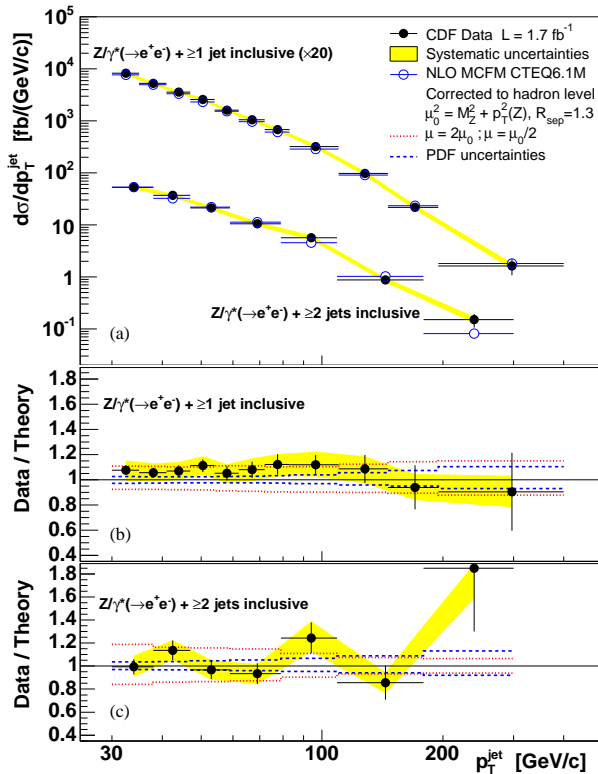


FIG. 15: Differential cross sections for  $Z/\gamma^*(\rightarrow e^+e^-) + 1$  or 2 jets at the Tevatron, as a function of  $p_T^{\text{jet}}$ , and in comparison with NLO theory [83]. Figure from ref. [82].

TABLE I:  $t\bar{t}$  forward-backward asymmetry at the Tevatron, from refs. [84, 86].

$A_{\text{FB}}^t(\%)$	$t\bar{t}$ inclusive	$t\bar{t}+\text{jet}$ inclusive	$t\bar{t}0\text{j}$ exclusive
LO	0	-6.9	0
NLO	3.8	$-1.5 \pm 1.5$	6.4

order,  $\mathcal{O}(\alpha_s^2)$ , just like the forward-backward asymmetry for muons in the QED process  $e^+e^- \rightarrow \mu^+\mu^-$ . But it is nonvanishing at NLO, or  $\mathcal{O}(\alpha_s^3)$  [85, 86, 87], as shown in table I. It is also nonvanishing for the process  $t\bar{t}+\text{jet}$ , computed at its leading order, again  $\mathcal{O}(\alpha_s^3)$ . Here a jet is required to have  $p_T^{\text{jet}} > 20$  GeV. Ref. [84] computed the asymmetry (7.1) in  $t\bar{t}+\text{jet}$  events at NLO,  $\mathcal{O}(\alpha_s^4)$ , and found the striking result that the asymmetry is drastically reduced, from  $-6.9\%$  to essentially zero. One might wonder what this result portends for the NNLO value of the  $t\bar{t}$  inclusive asymmetry — will it too receive a large correction?

In the mean time, the first forward-backward asymmetry measurements from the Tevatron were reported at

this conference. The observable used by CDF [6] and  $D\bar{O}$  [6, 88] is a bit different from eq. (7.1). It employs the rapidity difference between the  $t$  and  $\bar{t}$ ,

$$A^t = \frac{N_t(y_t > y_{\bar{t}}) - N_t(y_t < y_{\bar{t}})}{N_t(y_t > y_{\bar{t}}) + N_t(y_t < y_{\bar{t}})}. \quad (7.2)$$

The difference between these two observables for the NLO inclusive definition was studied recently [87]. For the same choice of pdfs, cuts, *etc.*, it is found that  $A_{\text{FB}}^t = (5.1 \pm 0.6)\%$ , whereas  $A^t = (7.8 \pm 0.9)\%$ . The observable  $A^t$  is somewhat larger than  $A_{\text{FB}}^t$  because events where both the  $t$  and  $\bar{t}$  go forward can contribute to  $A^t$  but not to  $A_{\text{FB}}^t$ .

CDF measures, with  $1.7 \text{ fb}^{-1}$  of data,

$$A^t = (28 \pm 13_{\text{stat}} \pm 5_{\text{syst}})\%; \quad (7.3)$$

while  $D\bar{O}$  measures, with  $0.9 \text{ fb}^{-1}$  of data,

$$A_{\text{uncorr}}^t = (12 \pm 8_{\text{stat}} \pm 1_{\text{syst}})\%, \quad (7.4)$$

the latter number has not been corrected for reconstruction effects. The statistical errors are still large, of course. However, in light of the large central values, it will certainly be interesting to follow these results as more data are analyzed.

## VIII. CONCLUSIONS

This talk has surveyed some of the recent progress over the past year or so in our quantitative theoretical understanding of hard QCD processes at colliders. An increasing number of processes are now known at NLO, and for a few benchmark processes, NNLO precision is available. Experiments at the Tevatron and at HERA test such QCD predictions over a wide range of kinematics. The experiment between experiment and theory is generally very good, except near kinematic boundaries such as small transverse momentum and small  $x$ , for which resummations and reorganizations of the perturbation theory should be performed. It is critical to push the “loops and legs” frontier to bring more processes to NLO and NNLO accuracy, and also to incorporate such processes into parton showers, while retaining that accuracy. But in general, we are “virtually” ready for the startup of the LHC next year!

## Acknowledgments

I am grateful to Z. Bern, D. Brown, M. Diehl, R. Erbacher, C. Gwenlan, J. Huston, M. Peskin, G. Salam and K. Tollefson for assistance in preparing this talk and write-up. I also thank the organizers of Lepton-Photon 2007 for the opportunity to present the talk at such a stimulating conference.

- 
- [1] A. Gehrmann-De Ridder, T. Gehrmann, E. W. N. Glover and G. Heinrich, Phys. Rev. Lett. **99**, 132002 (2007) [0707.1285 [hep-ph]]; 0710.0346 [hep-ph].
- [2] S. Bethke, Nucl. Phys. Proc. Suppl. **135**, 345 (2004) [hep-ex/0407021].
- [3] C. Gwenlan, “Deep inelastic scattering,” talk presented at LP07.
- [4] M. Diehl, “Implication of HERA measurements for LHC,” talk presented at LP07; 0711.1077 [hep-ph].
- [5] A. Rostovtsev, “Diffraction and vector meson production,” talk presented at LP07.
- [6] R. Erbacher, “Top quark properties,” talk presented at LP07.
- [7] D. J. Gross and F. Wilczek, Phys. Rev. Lett. **30**, 1343 (1973); H. D. Politzer, Phys. Rev. Lett. **30**, 1346 (1973).
- [8] V.N. Gribov and L.N. Lipatov, Yad. Fiz. **15**, 781 (1972) [Sov. J. Nucl. Phys. **15**, 438 (1972)]; G. Altarelli and G. Parisi, Nucl. Phys. B **126**, 298 (1977); Y.L. Dokshitzer, Sov. Phys. JETP **46**, 641 (1977) [Zh. Eksp. Teor. Fiz. **73**, 1216 (1977)].
- [9] S. Moch, J. A. M. Vermaseren and A. Vogt, Nucl. Phys. B **688**, 101 (2004) [hep-ph/0403192]; Nucl. Phys. B **691**, 129 (2004) [hep-ph/0404111].
- [10] A. Kanaki and C. G. Papadopoulos, Comput. Phys. Commun. **132**, 306 (2000) [hep-ph/0002082]; M. L. Mangano, M. Moretti, F. Piccinini, R. Pittau and A. D. Polosa, JHEP **0307**, 001 (2003) [hep-ph/0206293]; A. Cafarella, C. G. Papadopoulos and M. Worek, 0710.2427 [hep-ph].
- [11] K. Fabricius, I. Schmitt, G. Kramer and G. Schierholz, Z. Phys. C **11**, 315 (1981); H. Baer, J. Ohnemus and J. F. Owens, Phys. Rev. D **40**, 2844 (1989); J. Ohnemus and J. F. Owens, Phys. Rev. D **43**, 3626 (1991); W. T. Giele and E. W. N. Glover, Phys. Rev. D **46**, 1980 (1992); W. T. Giele, E. W. N. Glover and D. A. Kosower, Nucl. Phys. B **403**, 633 (1993) [hep-ph/9302225].
- [12] R. K. Ellis, D. A. Ross and A. E. Terrano, Phys. Rev. Lett. **45**, 1226 (1980), Nucl. Phys. B **178**, 421 (1981).
- [13] Z. Kunszt and D. E. Soper, Phys. Rev. D **46**, 192 (1992); G. Somogyi and Z. Trócsányi, hep-ph/0609041.
- [14] S. Frixione, Z. Kunszt and A. Signer, Nucl. Phys. B **467**, 399 (1996) [hep-ph/9512328].
- [15] S. Catani and M. H. Seymour, Phys. Lett. B **378**, 287 (1996) [hep-ph/9602277]; Nucl. Phys. B **485**, 291 (1997) [Erratum-ibid. B **510**, 503 (1998)] [hep-ph/9605323].
- [16] D. A. Kosower, Phys. Rev. D **57**, 5410 (1998) [hep-ph/9710213]; Phys. Rev. D **67**, 116003 (2003) [hep-ph/0212097]; Phys. Rev. D **71**, 045016 (2005) [hep-ph/0311272].
- [17] A. Daleo, T. Gehrmann and D. Maître, JHEP **0704**, 016 (2007) [hep-ph/0612257].
- [18] A. Gehrmann-De Ridder, T. Gehrmann and G. Heinrich, Nucl. Phys. B **682**, 265 (2004) [hep-ph/0311276].
- [19] C. Anastasiou, K. Melnikov and F. Petriello, Phys. Rev. D **69**, 076010 (2004) [hep-ph/0311311]; Phys. Rev. Lett. **93**, 032002 (2004) [hep-ph/0402280]; A. Lazopoulos, K. Melnikov and F. Petriello, Phys. Rev. D **76**, 014001 (2007) [hep-ph/0703273].
- [20] C. Anastasiou, K. Melnikov and F. Petriello, Nucl. Phys. B **724**, 197 (2005) [hep-ph/0501130].
- [21] T. Binoth and G. Heinrich, Nucl. Phys. B **585**, 741 (2000) [hep-ph/0004013]; G. Heinrich, Nucl. Phys. Proc. Suppl. **116**, 368 (2003) [hep-ph/0211144]; T. Binoth and G. Heinrich, Nucl. Phys. B **680**, 375 (2004) [hep-ph/0305234].
- [22] H. U. Bengtsson and T. Sjöstrand, Comput. Phys. Commun. **46**, 43 (1987); T. Sjostrand, P. Eden, C. Friberg, L. Lonnblad, G. Miu, S. Mrenna and E. Norrbin, Comput. Phys. Commun. **135**, 238 (2001) [hep-ph/0010017].
- [23] G. Marchesini and B. R. Webber, Cavendish-HEP-87/9; G. Marchesini, B. R. Webber, G. Abbiendi, I. G. Knowles, M. H. Seymour and L. Stanco, Comput. Phys. Commun. **67**, 465 (1992); G. Corcella *et al.*, hep-ph/0210213.
- [24] J. Alwall *et al.*, 0706.2569 [hep-ph].
- [25] S. Frixione and B.R. Webber, JHEP **0206**, 029 (2002) [hep-ph/0204244]; S. Frixione, P. Nason and B.R. Webber, JHEP **0308**, 007 (2003) [hep-ph/0305252].
- [26] P. Nason, JHEP **0411**, 040 (2004) [hep-ph/0409146]; P. Nason and G. Ridolfi, JHEP **0608**, 077 (2006) [hep-ph/0606275]; O. Latunde-Dada, S. Gieseke and B. Webber, JHEP **0702**, 051 (2007) [hep-ph/0612281]; S. Frixione, P. Nason and G. Ridolfi, JHEP **0709**, 126 (2007) [0707.3088 [hep-ph]].
- [27] S. Frixione, P. Nason and C. Oleari, 0709.2092 [hep-ph].
- [28] Z. Nagy and D. E. Soper, JHEP **0510**, 024 (2005) [hep-ph/0503053].
- [29] M. Dinsdale, M. Ternick and S. Weinzierl, Phys. Rev. D **76**, 094003 (2007) [0709.1026 [hep-ph]]; S. Schumann and F. Krauss, 0709.1027 [hep-ph].
- [30] W. T. Giele, D. A. Kosower and P. Z. Skands, 0707.3652 [hep-ph].
- [31] J. M. Campbell and R. K. Ellis, Phys. Rev. D **62**, 114012 (2000) [hep-ph/0006304]; <http://mcfm.fnal.gov/>
- [32] Z. Nagy, Phys. Rev. D **68**, 094002 (2003) [hep-ph/0307268]; <http://nagyz.web.cern.ch/nagyz/Website/NLOJET++/NLOJET++.html>
- [33] S. Catani, S. Dittmaier, M. H. Seymour and Z. Trócsányi, Nucl. Phys. B **627**, 189 (2002) [hep-ph/0201036].
- [34] T. Gleisberg and F. Krauss, 0709.2881 [hep-ph].
- [35] S. Weinzierl, JHEP **0303**, 062 (2003) [hep-ph/0302180]; S. Frixione and M. Grazzini, JHEP **0506**, 010 (2005) [hep-ph/0411399]; G. Somogyi, Z. Trócsányi and V. Del Duca, JHEP **0506**, 024 (2005) [hep-ph/0502226]; JHEP **0701**, 070 (2007) [hep-ph/0609042].
- [36] S. Catani and M. Grazzini, Phys. Rev. Lett. **98**, 222002 (2007) [hep-ph/0703012].
- [37] A. Gehrmann-De Ridder, T. Gehrmann and E. W. N. Glover, Nucl. Phys. B **691**, 195 (2004) [hep-ph/0403057]; Phys. Lett. B **612**, 36 (2005) [hep-ph/0501291]; Phys. Lett. B **612**, 49 (2005) [hep-ph/0502110]; JHEP **0509**, 056 (2005) [hep-ph/0505111].
- [38] J. C. Collins, D. E. Soper and G. Sterman, Nucl. Phys. B **250**, 199 (1985).
- [39] G. Sterman, Nucl. Phys. B **281**, 310 (1987); S. Catani and L. Trentadue, Nucl. Phys. B **327**, 323 (1989); Nucl. Phys. B **353**, 183 (1991).
- [40] S. Brandt, C. Peyrou, R. Sosnowski and A. Wroblewski, Phys. Lett. **12**, 57 (1964); E. Farhi, Phys. Rev. Lett. **39**, 1587 (1977).

- [41] A. Heister *et al.* [ALEPH Collaboration], *Eur. Phys. J. C* **35**, 457 (2004); S. Kluth, *Rept. Prog. Phys.* **69**, 1771 (2006) [hep-ex/0603011].
- [42] A. Gehrmann-De Ridder, T. Gehrmann, E. W. N. Glover and G. Heinrich, 0711.4711 [hep-ph].
- [43] G. Dissertori, A. Gehrmann-De Ridder, T. Gehrmann, E. W. N. Glover, G. Heinrich and H. Stenzel, 0712.0327 [hep-ph].
- [44] S. Dawson, *Nucl. Phys. B* **359**, 283 (1991); A. Djouadi, M. Spira and P. M. Zerwas, *Phys. Lett. B* **264**, 440 (1991); D. Graudenz, M. Spira and P. M. Zerwas, *Phys. Rev. Lett.* **70**, 1372 (1993); M. Spira, A. Djouadi, D. Graudenz and P. M. Zerwas, *Nucl. Phys. B* **453**, 17 (1995) [hep-ph/9504378].
- [45] F. Wilczek, *Phys. Rev. Lett.* **39**, 1304 (1977); M.A. Shifman, A.I. Vainshtein and V.I. Zakharov, *Phys. Lett. B* **78**, 443 (1978).
- [46] S. Catani, D. de Florian and M. Grazzini, *JHEP* **0105**, 025 (2001) [hep-ph/0102227]; R. V. Harlander and W. B. Kilgore, *Phys. Rev. D* **64**, 013015 (2001) [hep-ph/0102241]; *Phys. Rev. Lett.* **88**, 201801 (2002) [hep-ph/0201206]; C. Anastasiou and K. Melnikov, *Nucl. Phys. B* **646**, 220 (2002) [hep-ph/0207004]; V. Ravindran, J. Smith and W. L. van Neerven, *Nucl. Phys. B* **665**, 325 (2003) [hep-ph/0302135].
- [47] S. Catani, D. de Florian, M. Grazzini and P. Nason, *JHEP* **0307**, 028 (2003) [hep-ph/0306211].
- [48] S. Moch and A. Vogt, *Phys. Lett. B* **631**, 48 (2005) [hep-ph/0508265].
- [49] K. G. Chetyrkin, B. A. Kniehl and M. Steinhauser, *Nucl. Phys. B* **510**, 61 (1998) [hep-ph/9708255].
- [50] V. Ravindran, *Nucl. Phys. B* **752**, 173 (2006) [hep-ph/0603041]; V. Ravindran, J. Smith and W. L. van Neerven, *Nucl. Phys. B* **767**, 100 (2007) [hep-ph/0608308].
- [51] C. Anastasiou, G. Dissertori and F. Stöckli, *JHEP* **0709**, 018 (2007) [0707.2373 [hep-ph]].
- [52] C. Balazs, E. L. Berger, S. Mrenna and C. P. Yuan, *Phys. Rev. D* **57**, 6934 (1998) [hep-ph/9712471].
- [53] T. Binoth, J. P. Guillet, E. Pilon and M. Werlen, *Eur. Phys. J. C* **16**, 311 (2000) [hep-ph/9911340].
- [54] Z. Bern, L. J. Dixon and C. Schmidt, *Phys. Rev. D* **66**, 074018 (2002) [hep-ph/0206194].
- [55] P. Nadolsky, C. Balazs, E. L. Berger and C. P. Yuan, *Phys. Rev. D* **76**, 013008 (2007) [hep-ph/0702003].
- [56] C. Balazs, E. L. Berger, P. M. Nadolsky and C. P. Yuan, *Phys. Rev. D* **76**, 013009 (2007) [0704.0001 [hep-ph]].
- [57] D. E. Acosta *et al.* [CDF Collaboration], *Phys. Rev. Lett.* **95**, 022003 (2005) [hep-ex/0412050].
- [58] T. Han, G. Valencia and S. Willenbrock, *Phys. Rev. Lett.* **69**, 3274 (1992) [hep-ph/9206246].
- [59] T. Figy, C. Oleari and D. Zeppenfeld, *Phys. Rev. D* **68**, 073005 (2003) [hep-ph/0306109]; T. Figy and D. Zeppenfeld, *Phys. Lett. B* **591**, 297 (2004) [hep-ph/0403297].
- [60] M. Ciccolini, A. Denner and S. Dittmaier, *Phys. Rev. Lett.* **99**, 161803 (2007) [0707.0381 [hep-ph]]; 0710.4749 [hep-ph].
- [61] J. M. Campbell, R. K. Ellis and G. Zanderighi, *JHEP* **0610**, 028 (2006) [hep-ph/0608194].
- [62] R. K. Ellis, W. T. Giele and G. Zanderighi, *Phys. Rev. D* **72**, 054018 (2005) [Erratum-ibid. *D* **74**, 079902 (2006)] [hep-ph/0506196]; *Phys. Rev. D* **73**, 014027 (2006) [hep-ph/0508308].
- [63] W. Bartel *et al.* [JADE Collaboration], *Z. Phys. C* **33**, 23 (1986).
- [64] S. Catani, Y. L. Dokshitzer and B. R. Webber, *Phys. Lett. B* **285**, 291 (1992); S. Catani, Y. L. Dokshitzer, M. H. Seymour and B. R. Webber, *Nucl. Phys. B* **406**, 187 (1993); S. D. Ellis and D. E. Soper, *Phys. Rev. D* **48**, 3160 (1993) [hep-ph/9305266].
- [65] A. Abulencia *et al.* [CDF - Run II Collaboration], *Phys. Rev. D* **75**, 092006 (2007) [hep-ex/0701051].
- [66] J. M. Campbell, J. W. Huston and W. J. Stirling, *Rept. Prog. Phys.* **70**, 89 (2007) [hep-ph/0611148].
- [67] S. D. Ellis, J. Huston, K. Hatakeyama, P. Loch and M. Tönnesmann, 0712.2447 [hep-ph].
- [68] G. P. Salam and G. Soyez, *JHEP* **0705**, 086 (2007) [0704.0292 [hep-ph]].
- [69] J. Huston, <http://www.pa.msu.edu/~huston/SpartyJet/SpartyJet.html>
- [70] R. Akers *et al.* [OPAL Collaboration], *Z. Phys. C* **63**, 363 (1994); D. Buskulic *et al.* [ALEPH Collaboration], *Phys. Lett. B* **346**, 389 (1995); S. Behari *et al.* [AMY Collaboration], *Phys. Lett. B* **374**, 304 (1996); P. Abreu *et al.* [DELPHI Collaboration], *Eur. Phys. J. C* **4**, 1 (1998).
- [71] C. Adloff *et al.* [H1 Collaboration], *Nucl. Phys. B* **545**, 3 (1999) [hep-ex/9901010]; S. Chekanov *et al.* [ZEUS Collaboration], *Phys. Lett. B* **558**, 41 (2003) [hep-ex/0212030].
- [72] V. M. Abazov *et al.* [DØ Collaboration], *Phys. Rev. D* **65**, 052008 (2002) [hep-ex/0108054].
- [73] D. E. Acosta *et al.* [CDF Collaboration], hep-ex/0505013.
- [74] ZEUS Collaboration, ZEUS-prel-07-013, July 2007, preliminary results for Summer conferences.
- [75] DØ Collaboration, DØ Conference Note 5087, March 2007, preliminary results for Spring conferences.
- [76] N. Kidonakis and J. F. Owens, *Phys. Rev. D* **63**, 054019 (2001) [hep-ph/0007268].
- [77] CDF Collaboration, CDF/DOC/JET/PUBLIC/8928, July 2007, preliminary results for Summer conferences.
- [78] V. M. Abazov *et al.* [DØ Collaboration], *Phys. Rev. Lett.* **94**, 221801 (2005) [hep-ex/0409040].
- [79] H1 Collaboration, H1prelim-06-032, preliminary results submitted to DIS2006, April, 2006.
- [80] Z. Nagy and Z. Trócsányi, *Phys. Rev. Lett.* **87**, 082001 (2001) [hep-ph/0104315].
- [81] G. Hesketh [for the CDF and DØ Collaborations], hep-ex/0605073.
- [82] T. Aaltonen [CDF - Run II Collaboration], 0711.3717 [hep-ex].
- [83] J. Campbell and R. K. Ellis, *Phys. Rev. D* **65**, 113007 (2002) [hep-ph/0202176].
- [84] S. Dittmaier, P. Uwer and S. Weinzierl, *Phys. Rev. Lett.* **98**, 262002 (2007) [hep-ph/0703120].
- [85] F. Halzen, P. Hoyer and C. S. Kim, *Phys. Lett. B* **195**, 74 (1987); J. H. Kühn and G. Rodrigo, *Phys. Rev. Lett.* **81**, 49 (1998) [hep-ph/9802268]; *Phys. Rev. D* **59**, 054017 (1999) [hep-ph/9807420].
- [86] M. T. Bowen, S. D. Ellis and D. Rainwater, *Phys. Rev. D* **73**, 014008 (2006) [hep-ph/0509267].
- [87] O. Antunano, J. H. Kühn and G. V. Rodrigo, 0709.1652 [hep-ph].
- [88] V. M. Abazov *et al.* [DØ Collaboration], DØ Conference Note 5393, July 2007, preliminary results for Summer conferences.